Journal of Hazardous Materials 495 (2025) 138786

Contents lists available at ScienceDirect

Journal of Hazardous Materials

journal homepage: www.elsevier.com/locate/jhazmat

Acetamiprid in Rizhao green tea: Residue dynamics, degradation pathways, and ecological risks via integrated experimental and computational approaches

Changjian Li [a,*], Shujie Zhang [a], Chengcheng Han [a], Xiaolin Han [a], Jian Song [a], Jian Ju [c], Huimin Zhu [b,*]

[a] School of Public Health, Shandong Second Medical University, Weifang 261053, China
[b] School of Food Science and Technology, Jiangnan University, Wuxi 214122, China
[c] Special Food Research Institute, Qingdao Agricultural University, Qingdao 266109, China

HIGHLIGHTS

- Integrated field-computational study on acetamiprid fate in tea ecosystems.
- Seasonal harvest strategies proposed to minimize pesticide residues.
- Drying process identified as critical for residue concentration control.
- Degradation of products is linked to chronic aquatic ecological risks.

GRAPHICAL ABSTRACT

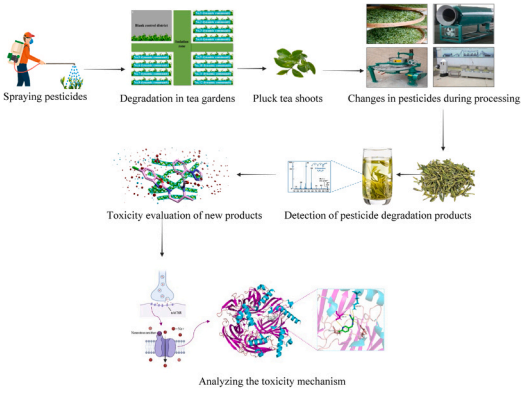

ARTICLE INFO

Keywords:
Pesticides
Green tea
Drying
Processing factor
Toxicity

ABSTRACT

This study assesses the environmental persistence, processing effects, and toxicity mechanisms of acetamiprid in Rizhao green tea. Uniquely, we integrate season-resolved field trials, full-scale factory processing and atomistic DFT–docking analyses to deliver the first "field-to-cup" mass-balance for any neonicotinoid in tea. Field trials demonstrated concentration-dependent dissipation kinetics, with half-lives decreasing from 5.54 days (spring, RD) to 4.36 days (autumn, 3 ×RD). Seasonal variations, driven by higher autumn temperatures (18.2 °C vs. 12.5 °C) and light intensity (PAR: 1451 vs. 982 μmol/m²/s), significantly accelerated acetamiprid degradation. During tea processing, fixation reduced residues (*PF*<1), while drying caused significant accumulation (*PF* 2.63–2.99) due to high vapor pressure. GC-MS identified six degradation products, two of which—6-chloronicotinaldehyde and methyl 6-chloronicotinate—showed chronic toxicity to aquatic organisms (EC_{50}: 45.2–62.7 mg/L), though acute toxicity was absent. Density functional theory (DFT) revealed reactive sites in acetamiprid's side chain, aligning with hydrolysis/oxidation pathways. Molecular docking and dynamics simulations elucidated

* Corresponding authors.
E-mail addresses: licj667@sdsmu.edu.cn, amtfa88@163.com (C. Li), zhmsky@126.com (H. Zhu).

https://doi.org/10.1016/j.jhazmat.2025.138786
Received 2 April 2025; Received in revised form 18 May 2025; Accepted 29 May 2025
Available online 30 May 2025

acetamiprid's neurotoxic mechanism: stable binding to nAChRs via hydrogen bonds with Trp-86 (−12.5 ± 0.8 kcal/mol contribution) and Lys-10, yielding a spontaneous binding energy of −5.5 kcal/mol. Seasonal harvesting adjustments (prolonged spring intervals) and optimized drying protocols are proposed to minimize residues. The study underscores the ecological risks of acetamiprid's environmental persistence (soil half-life: 6.3–9.5 days) and transformation products, advocating for integrated agronomic practices to safeguard tea quality and aquatic ecosystems.

1. Introduction

The selection of green tea in China is diverse and vibrant, featuring Rizhao green tea, a product of Rizhao City, recognized as one of the world's three coastal green tea metropolises [1]. Additionally, the local tea in this area is rich in nutrients such as tea polyphenols, theanine, and flavonoids due to the region's unique climatic factors [2–4]. However, tea trees face various diseases and insect pests that cause the yield of tea gardens to decrease by approximately 10 –20 % annually. To ensure the quality of green tea, China's Ministry of Agriculture has explicitly banned the use of highly toxic and persistent pesticides in tea plantations [5,6]. Consequently, acetamiprid, a new nicotine broad-spectrum insecticide with low toxicity and high efficacy, is widely used in green tea cultivation [7,8]. Although acetamiprid dissipates rapidly under ideal field conditions , nationwide surveillance of 726 Chinese teas reported residues in 73 % of samples [9] , and a targeted survey of 105 retail green-tea samples from Hangzhou still detected acetamiprid in 26.7 % of cases [10]. In March 2025, the RASFF (Rapid Alert System for Food and Feed) alert further confirmed acetamiprid (1.1 mg kg^{-1}) in mixed-origin teas entering the EU [11]. Field-level evidence points to behavioural causes: surveys of 786 smallholders in Shaanxi, Sichuan, Zhejiang and Anhui revealed that short harvesting cycles and risk-averse attitudes drive many growers to harvest before the recommended pre-harvest interval (PHI) and to apply insecticides at rates exceeding the label instructions [12]. Industry reviews likewise document systematic over-application of pesticides in conventional tea ecosystems [13]. These real-world observations expose a clear gap between laboratory dissipation kinetics and commercial residue occurrence.

Acetamiprid exhibits both rapid and long-lasting insecticidal effects, making it a commonly used pesticide for controlling leafhoppers, thrips, aphids, and other pests in green tea cultivation [14,15]. Despite its efficacy in enhancing agricultural yields, widespread use of acetamiprid raises significant concerns due to its persistence in the environment and potential health hazards. Long-term residues of acetamiprid in the environment pose a threat to aquatic ecosystems, affecting the health of fish, amphibians and benthic organisms through accumulation in the food chain [16–18]. In addition, acetamiprid is toxic to pollinating insects such as bees, causing a significant decline in the bee population, which in turn affects the plant pollination process and threatens biodiversity and the stability of agricultural ecosystems [19,20]. Environmental factors degrade and transform the potential pesticide residues on the tea surface. As a result, the original pesticides and their transformed products may coexist in the environment [21,22]. Yeter et al. (2020) found that acetamiprid is degraded in animals mainly by N-demethyl acetamiprid (IM-2–1) [23], whereas Popadić et al. (2023) found that the zeolite-catalysed thermal degradation of acetamiprid mainly involves cleavage of the C-C bond between the aromatic core of the molecule and its tail end, followed by cleavage of the C-N bond [24]. It is crucial to consider that certain converted substances may possess distinct types or even greater levels of toxicity compared to their parent pesticides. For instance, dichlorvos, derived from trichlorfon, is about eight times more toxic than trichlorfon [25,26]. Therefore, the assessment of pesticide risks should incorporate the potentially hazardous effects of conversion products.

The degradation rates of pesticides in the environment are significantly influenced by their physical and chemical properties, including photosensitivity, water solubility, and vapor pressure [27,28]. Water-soluble pesticides are susceptible to loss through rainfall; however, their impact can be mitigated if they exhibit strong internal absorption [29]. In addition, light-sensitive pesticides may undergo molecular structural cleavage or isomerization upon exposure to sunlight. These pesticides can indirectly promote photolysis by absorbing energy transferred by photosensitizers [30]. Rizhao green tea, cultivated in a coastal temperate monsoon climate with acidic soil (pH 5.2 ± 0.3), exhibits distinct physicochemical interactions with acetamiprid residues compared to other tea varieties. Research indicates that under precipitation conditions, 22–49 % of pesticides can be washed away from tea surfaces [31]; for example, imidacloprid exhibits a longer half-life during dry seasons than during wet seasons [32]. The residual time on plant leaves also depends on the pesticide dosage. For example, the half-life of deltamethrin at twice the recommended dose is 0.5 days longer than the half-life at the lower recommended dose [33]. Moreover, pesticide not only gradually dissipates under natural conditions but also undergoes changes in residue levels during tea processing. For example, the spreading process promotes the photolysis and co-distillation of nicotine pesticides, consequently leading to reduced levels of pesticide residues in withered tea [34].

Building on the unresolved safety questions surrounding neonicotinoids in tea, this study is designed to trace acetamiprid from field to cup—linking its seasonal dissipation in Rizhao tea gardens with residue behaviour at each processing stage (spreading→ fixation→rolling→drying) and the potential hazards of the compounds formed along the way. By coupling long-term field trials with GC-MS metabolite mapping and mechanism-oriented DFT and molecular-docking analyses, we establish an integrated experimental–computational platform that has not yet been applied to any tea system. The work therefore aims to fill critical knowledge gaps on how cultivation conditions and industrial thermal treatments together shape acetamiprid's environmental fate and toxicological profile, providing a scientific basis for safer pesticide use, process optimisation and ecological risk management in green-tea production.

2. Materials and methods

2.1. Chemicals

Acetamiprid soluble concentrate (20 % active ingredient, a.i.) was supplied by Shandong Zouping Pesticide Co., Ltd. (Binzhou, China). Acetamiprid, 6-chloronicotinaldehyde, methyl 6-chloronicotinate analytical standard (purity ≥98.0 %), deuterated internal standard (acetamiprid-d_3, purity ≥98.0 %), and dichlorodihydrofluorescein diacetate (DCFH-DA) were purchased from Sigma-Aldrich (St. Louis, MO, USA). Chromatographic-grade solvents, including acetonitrile, acetone and n-hexane were obtained from Merck KGaA (Darmstadt, Germany). Sodium chloride, anhydrous magnesium sulfate, and formic acid were of analytical grade and sourced from Sinopharm Chemical Reagent Co., Ltd. (Beijing, China). *Chlorella vulgaris* (strain SAG 211–11b, obtained from the Guangyu, China) was pre-cultured in BG-11 medium (Sigma-Aldrich, St. Louis, MO, USA).

For sample purification, primary secondary amine (PSA, 40–60 μm) and graphitized carbon black (GCB, 120–400 mesh) were procured from Agela Technologies (Tianjin, China). Ceramic homogenizers (2.8 mm diameter) and 0.22 μm nylon membrane filters were supplied by Shanghai Xinya Purification Material Co., Ltd (Shanghai, China).

Ultrapure water (resistivity ≥18.2 MΩ·cm) was prepared using a Milli-Q Integral Water Purification System (Merck Millipore, Billerica, MA, USA).

2.2. Field experiment design

2.2.1. Experimental site and conditions

The field trial was conducted in Houcun Town, Rizhao City, Shandong Province, China (35°23′N, 119°32′E), during the spring (March–May 2021) and autumn (June–September 2022) tea-growing seasons. The region is characterized by a temperate monsoon climate with an average annual temperature of 12.7 °C and rainfall of 768.7 mm. The experimental plots were established in tea gardens with uniform soil properties (pH 5.2 ± 0.3, organic matter 2.8 ± 0.2 %) and consistent cultivation practices.

2.2.2. Pesticide application

Refer to Fig. 1a for specific details on the experimental design. Acetamiprid (soluble concentrate, 20 % a.i., Shandong Zouping Pesticide Co., China) was applied at three dose levels:

(1) Recommended dose (RD): 22.5 g a.i./ha (equivalent to 112.5 g commercial product/ha).
(2) Double recommended dose (2 ×RD): 45 g a.i./ha.
(3) Triple recommended dose (3 ×RD): 67.5 g a.i./ha.

To capture a realistic worst-case boundary for the residue and risk assessment, the three-tier scheme (1 ×, 2 ×, 3 × RD) was adopted in accordance with OECD Guideline No. 132, which states that application levels "two-fold or more above the recommended rate should be employed when establishing a risk margin" [35].

Control plots received equivalent volumes of water to account for solvent effects. A motorized backpack sprayer (3WBD-16, Shandong, China) equipped with a hollow-cone nozzle was used to ensure uniform foliar application. Spraying was performed under wind speeds < 2 m/s and temperatures < 30 °C to minimize drift and volatilization. Each treatment was replicated four times (plot size: 10 m^2), with untreated plots serving as controls.

2.2.3. Sampling strategy

Fresh tea leaves: Samples (≥500 g) were collected from each plot at

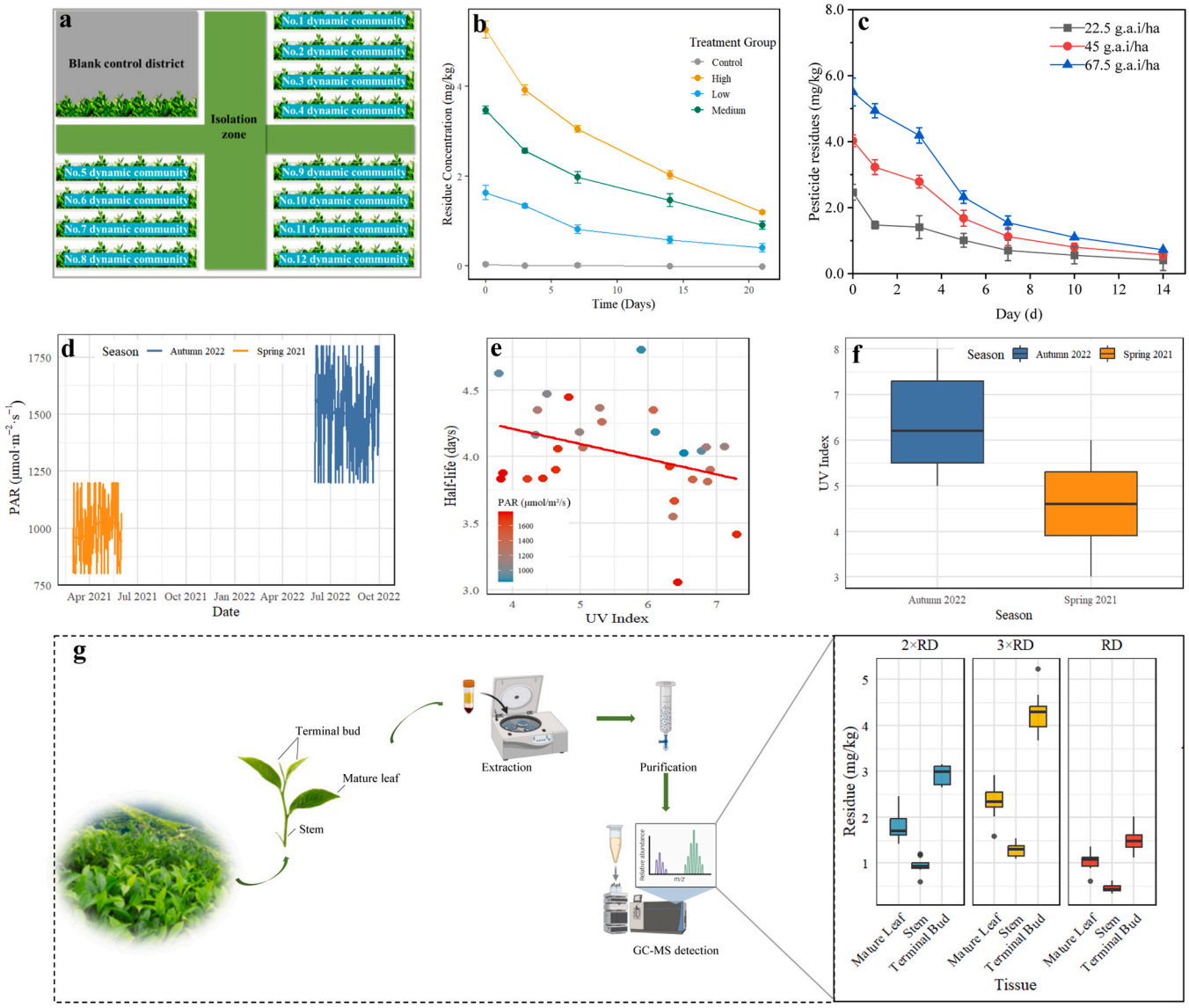

Fig. 1. Design drawing of the experimental district (a); the degradation kinetic model of acetamiprid in soil (b) and tea (c); the impact of light intensity during the experiment (d), the effect of UV index on acetamiprid half-life (e), seasonal variations in UV Index (f), and a comparison of pesticide residue levels in different parts of tea plants (g).

1, 3, 5, 7, 10, and 14 days after application (DAA) [36]. To assess acropetal translocation, leaves were categorized into: (1) Terminal buds (youngest fully expanded leaf); (2) 1st mature leaf (immediately below the bud) and 2 nd mature leaf (lower canopy); (3) Stems.

Soil samples: To evaluate the migration and persistence of acetamiprid in the soil ecosystem, soil cores (0–20 cm depth) were collected from each plot at 0, 3, 7, 14, and 21 DAA. Three replicate cores were randomly collected within a 1 m radius of tea bushes. Samples were air-dried, homogenized, and sieved through a 2-mm mesh for residue analysis.

2.2.4. Environmental monitoring

Ultraviolet index (UVI, 280–400 nm) and photosynthetically active radiation (PAR, 400–700 nm) were continuously monitored using a CUV5 radiometer (Kipp & Zonen, Netherlands) and LI-190R quantum sensor (LI-COR, USA) respectively. Both sensors, mounted 1.5 m above the tea canopy, were connected to a CR1000 datalogger (Campbell Scientific, USA) recording measurements at 1-minute intervals. Daily averages were calculated from 24-hour continuous data after excluding periods of instrumental malfunction or precipitation.

2.3. Green tea processing method

Fresh tea leaves harvested 24 hours post-pesticide application were processed into Rizhao green tea (GB/T 32744–2016) through a four-stage protocol. The process began with dual spreading methods: natural spreading (10–15 °C, 70–75 % RH, 5 h) reduced moisture to 71.8 %, while mechanical spreading using a YS-6CTQ-120 machine (Hongte, China) at 16–20°C achieved 70 % moisture. Fixation was then performed in a 60-drum continuous machine (Anxi Nandan, China) at 220–260°C for 2 min, monitored by Fluke 62 Max infrared thermometer to maintain 85–90°C leaf temperature, achieving > 95 % polyphenol oxidase (PPO) deactivation. Rolling followed using a 6CR-45 roller (Junlai, China) for 15–25 min to attain 45–65 % cell disruption. Drying involved two phases: primary drying in a 60-T tea fryer (Junlai, China) at 90–110°C (30–50 min, 10 % moisture) and final aroma stabilization at 80°C for 20 min.

2.4. Detection method for acetamiprid

2.4.1. Sample preparation

Tea Samples followed a modified version of the Chinese National Standard Method GB/T 23204–2008. Fresh tea leaves (2.0 g) were weighed into a 50 mL centrifuge tube. Acetonitrile (20 mL) was added, and the mixture was vortexed for 1 min and allowed to stand for 15 min. Subsequently, sodium chloride (1 g) and anhydrous magnesium sulfate (1 g) were added, vortexed (Vortex-2, IKA, Germany) for 1 min, and centrifuged at 8000 rpm for 5 min. The supernatant (10 mL) was collected in a round-bottom flask and rotary-evaporated to near dryness. The residue was purified using a homemade florisil + GCB hybrid column pre-wetted with 5 mL of acetone-hexane (1:1). The column was eluted three times with 15 mL of acetone-hexane (1:1). The eluate was concentrated to near dryness, reconstituted in 1 mL acetonitrile, and transferred to a 2 mL centrifuge tube containing 30 mg PSA and 30 mg GCB. After vortexing (30 s) and centrifugation (12,000 rpm, 1 min), the supernatant was filtered through a 0.22 μm membrane prior to analysis.

Soil samples were air-dried, homogenized, and sieved through a 2-mm mesh. For extraction, 10 g of soil was mixed with 10 mL acetonitrile, 1 g NaCl, and 4 g $MgSO_4$. The mixture was vortexed for 1 min, centrifuged at 8000 rpm for 5 min, and purified using the same PSA + GCB column procedure as described for tea samples. Final extracts were filtered through a 0.22 μm membrane.

2.4.2. Instrumental analysis

Acetamiprid residues in both tea and soil extracts were analyzed using a gas chromatography-mass spectrometry system (GC-MS-QP2020, Shimadzu, Japan) equipped with a DB-5MS capillary column (30 m × 0.25 mm × 0.25 μm, Agilent, USA). Carrier gas: helium, purity ≥ 99.9 %; mass spectrometry conditions: ion source temperature 230 ℃; GC-MS interface temperature, 280 ℃; inlet temperature, 290 ℃, flow rate, 1.2 mL/min. The injection volume was 1 μL, utilizing a non-split injection technique. The programmed temperature rise followed this sequence: 40 ℃ for 1 min, a rapid temperature increase of 30 ℃/min to reach 130 ℃, followed by a more gradual 5 ℃/min temperature increase to 250 ℃. The final phase involved a rapid 10 ℃/min increase to 300 ℃, sustained for 5 min. Throughout this process, the instrument operated in full scan mode, scanning within the range of m/z 50–500.

2.4.3. Method validation

Validation was performed according to GB/T 23204–2008. For tea matrices, recoveries of acetamiprid ranged from 93–96 % with relative standard deviations (RSD) of 3.7–5.3 % (n = 6). Soil analysis showed recoveries of 89–94 % (RSD < 6 %, n = 3). The limit of quantification (LOQ) was 0.012 mg/kg for both matrices.

2.4.4. Statistical analysis

The kinetic formula of pesticide residue digestion is as follows:

$$C_t = C_0 e^{-kt}$$

$$t_{1/2} = ln2/k$$

where k is the pesticide dissipation coefficient, t is the application time (days), $t_{1/2}$ is the half-life (days), C_t is the amount of pesticide residue at time t (mg/kg), and C_0 is the initial amount of pesticide deposited after application (mg/kg).

Tea water content and dry matter rate are expressed as mass fractions (%), and dry matter pesticide residue (mg/kg) refers to the actual amount of pesticide residue in the tea after correcting for the tea water content. The formulas for calculating the dry matter rate and dry matter residue are as follows:

$$W_d = 1\text{-}W$$

$$C_d = C/W_d$$

where W is the water content (%), W_d is the dry matter content (%), C is the pesticide concentration (mg/kg), and C_d is the actual amount of pesticide residue in the tea after correcting for the water content (mg/kg).

In this study, the processing factor (PF) was used to reflect the changes in pesticide degradation during processing, calculated as follows:

$$\mathrm{PF} = \frac{C_2}{C_1}$$

C_1 refers to the measured pesticide residue level of the sample in the previous process (mg/kg), and C_2 refers to the measured pesticide residue level of the sample after processing (mg/kg). If $PF > 1$, it signifies that the process has an enrichment effect on the measured pesticide; if $PF < 1$, it indicates that the process causes the pesticide residue level to decrease.

The data obtained in the experiments were expressed using mean values ± standard deviation (x ± SD), and each experiment was repeated three times under the same conditions. Graphs were plotted using Origin 2021 software, analyzed by ANOVA using IBM SPSS Statistics, and compared using the letter-labeling method. $P < 0.05$ indicates a significant difference between experimental samples.

2.5. Computational analysis of acetamiprid's molecular reactivity

The electronic structure optimization of acetamiprid was performed through density functional theory computations (M06–2X/6–311 G d,p

basis set) implemented in Gaussian16 software [37]. Geometry optimizations employed tight convergence criteria (maximum force < 0.00045 Hartree/Bohr, RMS displacement < 0.0018 Å), and vibrational frequency analysis confirmed the absence of imaginary frequencies, ensuring optimized structures corresponded to energy minima. An ultrafine integration grid (99,590 points) was applied for precise electron density evaluation. Quantum chemical calculations were conducted to determine critical electronic characteristics including frontier molecular orbitals and electrostatic potential distribution, which provide theoretical insights into reactive site identification.

2.6. Toxicity assessment

2.6.1. ECOSAR

The toxicity of acetamiprid and its degradation products was predicted using the ECOSAR (version 2.2) program developed by the U.S. Environmental Protection Agency [38]. The QSAR models for acute toxicity (e.g., 96-h LC_{50} for fish, 48-h EC_{50} for Daphnia) and chronic toxicity (21-day NOEC for aquatic organisms) were selected based on the molecular structures, following the Globally Harmonized System of Classification and Labelling of Chemicals (GHS). The predictions covered key ecological receptors, including freshwater fish (Oncorhynchus mykiss), water flea (Daphnia magna), and green algae (Pseudokirchneriella subcapitata), with model validation criteria (e.g., applicability domain, goodness-of-fit) referenced from prior studies [39].

2.6.2. Chlorella vulgaris

Chlorella vulgaris (SAG 211–11b) was pre-cultured in BG-11 medium under controlled conditions (25 ± 1°C, 80 μmol/m²/s light intensity, 16:8 h light/dark cycle) until reaching the logarithmic growth phase ($OD_{680} \approx 0.2$). Algal cells were then resuspended to an initial density of 1×10^5 cells/mL. Concentration gradients of acetamiprid (0.1–100 mg/L), 6-chloronicotinaldehyde (product b, 0.01–10 mg/L), and methyl 6-chloronicotinate (product c, 0.01–10 mg/L) were established, with three replicates per group, along with acetone solvent controls (final concentration ≤0.1 % v/v) and blank medium controls. After 72-hour exposure, cell density was measured spectrophotometrically (OD_{680}) to calculate growth inhibition rates. Chlorophyll a content was quantified via acetone extraction (OD_{663}/OD_{645}), and reactive oxygen species (ROS) levels were detected using the fluorescent probe DCFH-DA with a microplate reader (Ex/Em= 485/535 nm).

2.6.3. Molecular docking

The binding mechanism of acetamiprid to the Apis mellifera nAChR α8 subunit (PDB ID: 4zk4) was investigated using AutoDock Vina 1.1.2 [40]. Bee-specific nicotinic acetylcholine receptors are recognised as the primary molecular targets of neonicotinoids and are explicitly listed as indicator proteins in the EFSA bee-risk guidance [41]. The receptor structure was preprocessed by removing crystallographic water molecules, adding polar hydrogens, and assigning Gasteiger charges. A grid box (40 ×40 ×40 Å³) centered on the ligand-binding pocket (x = 15.2, y = 22.7, z = 18.4) was generated to encompass key residues. The acetamiprid structure was energy-minimized with the MMFF94 force field in Sybyl-X 2.0 (RMSD gradient <0.05 kcal/mol·Å) [42]. Docking simulations were performed with an exhaustiveness of 20, generating 50 conformations. The lowest-energy pose was selected, and interactions were visualized in PyMOL 2.5.

2.6.4. Molecular dynamics simulations

The stability of the acetamiprid-nAChR complex was evaluated through 50 ns MD simulations using GROMACS 2022.4. The system was solvated in a TIP3P water box (1.2 nm padding) and neutralized with Na^+ ions. Energy minimization was performed via the steepest descent algorithm, followed by NVT and NPT equilibration (300 K, 1 bar). Production runs utilized the AMBER ff19SB force field for the receptor and GAFF2 for acetamiprid. Trajectories were analyzed for RMSD, RMSF, and hydrogen bonding using built-in GROMACS tools.

2.6.5. MM/PBSA binding free energy calculation

Binding free energy was calculated from 500 snapshots extracted at 100 ps intervals using the g_mmpbsa tool. The polar solvation term was computed via the Poisson-Boltzmann equation (grid spacing = 0.5 Å), while the non-polar term was derived from the SASA model. Energy decomposition identified key residue contributions.

3. Results and discussion

3.1. Residue dissipation dynamics in tea leaves and soil

The dissipation of acetamiprid in both tea leaves and soil conformed to first-order kinetics (Fig. 1b-c and Table 1). On tea leaves, the half-life gradually decreased from 5.54 to 4.36 days as application concentrations increased from 22.5 to 67.5 g a.i./ha (R^2 =0.89–0.97), suggesting concentration-dependent degradation. Notably, this degradation rate was significantly faster than that observed in strawberries (6.9–8.1 days) [43], likely due to the thin leaves and large specific surface area of tea plants, which enhance photodegradation and volatilization.

The degradation rate constants (k) in soil (k_soil = 0.073–0.110 day^{-1}) were 23–37 % lower than those in tea leaves (k_tea = 0.125–0.159 day^{-1}), indicating slower dissipation ($p < 0.05$). This discrepancy can be attributed to limited photolysis and reduced microbial activity in the subsurface environment [44]. Dose-dependent accumulation was evident in both matrices: at the recommended dose (22.5 g a.i./ha), residues in tea leaves decreased from 1.01 mg/kg (Day 5) to 0.7 mg/kg (Day 7), while soil residues declined from 1.45 mg/kg to 0.32 mg/kg over 21 days. Triple-dose applications exacerbated soil persistence, with 38 % of initial residues (3.89 mg/kg) remaining after 21 days.

3.2. Seasonal and environmental drivers

Acetamiprid degradation exhibited strong seasonal variation. In tea leaves, the half-life was significantly shorter in autumn (2.36–4.81 days) than in spring (4.65–5.54 days) (Table 1), correlating with higher autumn temperatures (18.2 ± 2.1°C vs. 12.5 ± 1.8°C) and light intensity (Fig. 1d-f, PAR: 1451 ± 200 vs. 982 ± 150 μmol/m²/s). Soil degradation also accelerated in autumn, with 12 % shorter half-lives compared to spring, likely driven by elevated soil moisture (15–18 % vs. 10–12 %) and microbial biomass [45]. These findings suggest that seasonal plucking schedules could optimize residue management—prolonging harvest intervals in spring may enhance degradation, whereas autumn's natural climatic advantages reduce persistence risks.

Table 1
Degradation of dynamic equation, correlation coefficient and half-life of acetamiprid residue test in the field.

Initial concentration (g.a.i/ha)	Dispelling dynamic equation	R^2	$t_{1/2}$ (d)
22.5[a]	$C_t = C_0\, e^{-0.125t}$	0.91	5.54
	$C_t = C_0\, e^{-0.096t}$	0.95*	7.20*
45.0[a]	$C_t = C_0\, e^{-0.139t}$	0.97	4.99
	$C_t = C_0\, e^{-0.086t}$	0.92*	8.10*
67.5[a]	$C_t = C_0\, e^{-0.149t}$	0.96	4.65
	$C_t = C_0\, e^{-0.073t}$	0.91*	9.50*
22.5[b]	$C_t = C_0\, e^{-0.144t}$	0.89	4.81
	$C_t = C_0\, e^{-0.110t}$	0.93*	6.30*
45.0[b]	$C_t = C_0\, e^{-0.146t}$	0.97	4.74
	$C_t = C_0\, e^{-0.098t}$	0.90*	7.10*
67.5[b]	$C_t = C_0\, e^{-0.159t}$	0.97	4.36
	$C_t = C_0\, e^{-0.083t}$	0.89*	8.40*

* Soils;
[a] spring;
[b] autumn.

3.3. Acropetal translocation and tissue-specific accumulation

A pronounced dose-dependent accumulation gradient was observed across tea tissues (Fig. 1g). Terminal buds retained the highest residues (4.2 ± 0.5 mg/kg under 3 ×RD), followed by mature leaves (2.5 ± 0.4 mg/kg) and stems (1.2 ± 0.3 mg/kg), confirming systemic acropetal translocation via xylem. The translocation factor (TF = bud/stem residue ratio) increased from 3.0 (RD) to 3.5 (3 ×RD), highlighting dose-dependent enrichment in metabolically active tissues. This aligns with the chemical's nicotine acetylcholine receptor (nAChR) affinity, which facilitates uptake and vascular transport [46].

3.4. Environmental fate and risk implications

The environmental persistence of acetamiprid raises significant ecological and agricultural concerns. Prolonged soil half-lives (6.3–9.5 days), combined with high annual rainfall (>700 mm in Rizhao), elevate leaching risks, particularly under triple-dose applications where soil residues exceed 1.2 mg/kg for over two weeks. Although residues remained below the recommended threshold for agricultural soils (0.1 mg/kg) [47], repeated applications may lead to cumulative contamination. Furthermore, chronic exposure to soil residues poses ecotoxicological risks, as evidenced by studies showing disruptions to microbial communities and earthworm populations under neonicotinoid exposure[48]. Using these PECs (Predicted Environmental Concentrations) with the measured Daphnia magna 48 h LC_{50} of 5.8 μg L^{-1} yielded risk quotients (RQ) of 0.21 (spring) and 0.12 (autumn), classifying the acute aquatic risk as low (< 0.5), whereas the chronic algal ChV of 1.0 μg L^{-1} produced an RQ of 1.18, signalling moderate concern for primary producers during early-season runoff. These dual risks—groundwater contamination and soil ecosystem disruption—underscore the urgency of integrating agronomic practices such as organic fertilization (to enhance microbial degradation) with strict dose optimization. Future research should prioritize mechanistic models to predict the multi-media fate of acetamiprid under climate change scenarios, alongside long-term field monitoring to validate mitigation strategies.

3.5. Effect of green tea processing on acetamiprid residues

The initial step in green tea processing is referred to as "spreading." During this stage, tea buds undergo a series of physical and chemical changes. Moderate spreading has the capacity to release green grass gas, unveil the fragrance, facilitate the formation of favorable aroma substances, and improve the quality of the finished tea.

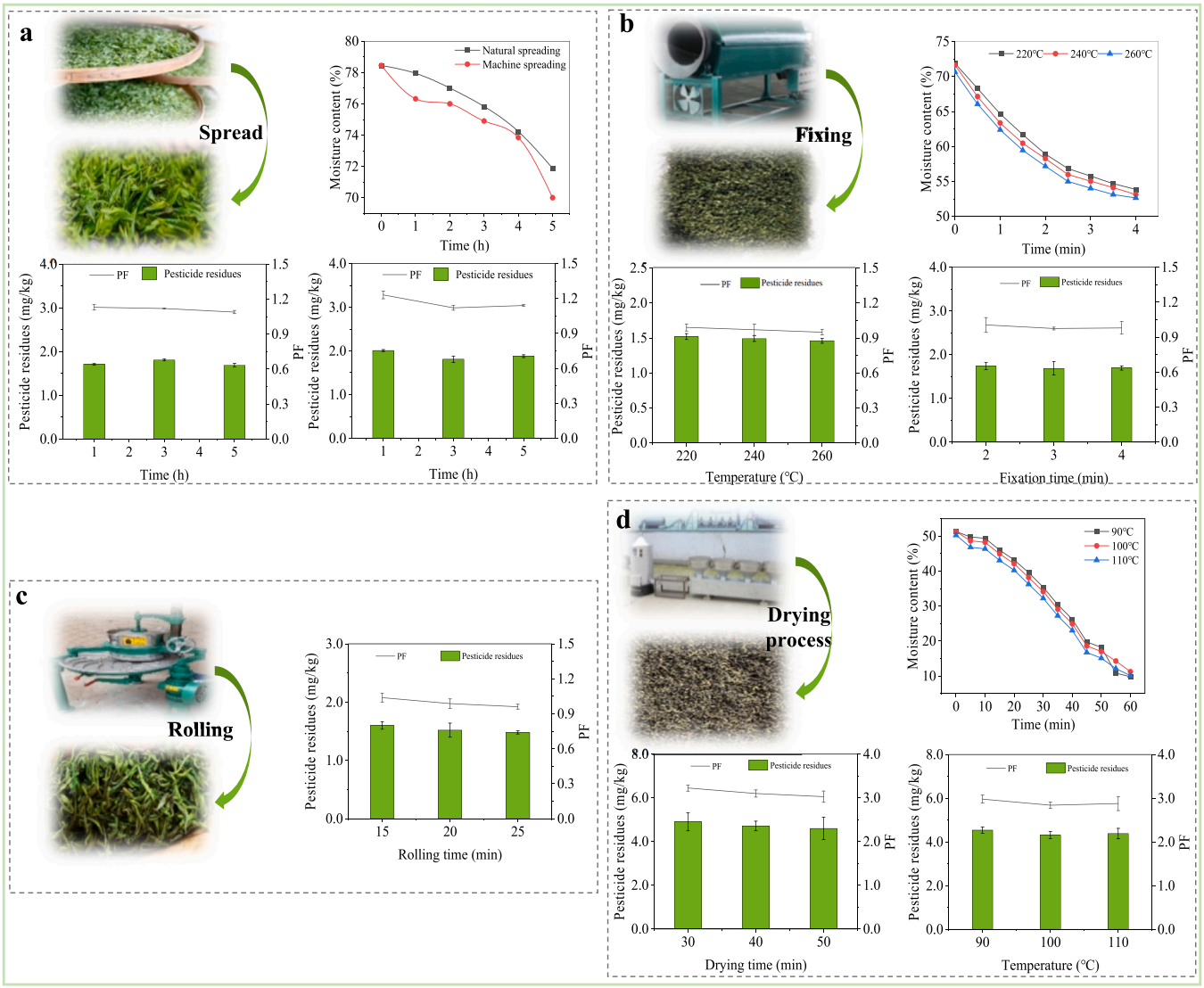

Fig. 2. The variation of acetamiprid residue levels and *PF* during different stages of processing tea shoots into dry tea (a, spread; b, fixing; c, rolling; d, drying process).

In the technological realm of green tea processing, spreading tea buds for 4–8 hours, maintaining a moisture content of 70–72 %, proves to be the most appropriate, resulting in the highest quality of finished tea. As shown in Fig. 2a, the leaves lost water continuously during the spreading process, and the moisture content decreased to 71.8 % and 70 % after 5 h of natural and machine spreading, respectively. Meanwhile, the residues of acetamiprid were 1.75 mg/kg and 1.69 mg/kg following natural and machine spreading, respectively. Meanwhile, the *PF* ranged from 1.09–1.14, which indicated that the spreading process had less influence on the pesticide residues. However, the *PF* was slightly lower following the machine spreading process compared to natural spreading. This may be due to the fact that machine spreading has heating and exhausting functions, facilitating more efficient water evaporation. This result is consistent with the findings of Peng-cheng [49], who demonstrated that machine spreading exhibits higher water loss efficiency. However, it has been shown that the degree of residue change during spreading may also be related to pesticide species. For example, the residue of deltamethrin may decrease because of its volatilization during prolonged spreading [50].

Fixation is not only the second step in green tea processing but also a key process in shaping the quality of green tea. Fixation involves implementing high-temperature measures to distribute water in the leaves, passivating the activity of enzymes, and making certain chemical changes to the contents of fresh leaves to form the quality characteristics of green tea. As shown in Fig. 2b, the spread green tea is treated in a cylindrical water-removing machine at 220–260 ℃. This treatment resulted in a rapid decrease in the water content of leaves and an increase in the dry matter content from 28.1–29.4 % to 46.2–47.4 %. At the same time, the residue range of acetamiprid was measured at 1.45–1.54 mg/kg, and its *PF* decreased to 0.95 with the rise in fixation temperature, indicating that acetamiprid was degraded partially.

Rolling is the third step in green tea processing, aiming to shape fresh tea leaves into strips, particles, and other required shapes. During the rolling process, tea cells break, causing cell fluid to overflow and attach to the surface of the formed green tea. This contributes to the color and taste of green tea when brewed after drying. Typically, a cell damage rate between 45 % and 65 % is required. According to the results shown in Fig. 2c, the *PF* ranged between 0.96–1.04 under different rolling times. Notably, because rolling does not require heating, it has little effect on pesticide residues. In addition, although rolling is similar to spreading, the changes in pesticide residues are not obvious; therefore, rolling is not the primary process influencing pesticide degradation.

Drying is the fourth step of green tea processing. Through drying, the moisture in tea leaves can be removed for storage and the formation of quality characteristics, such as color and aroma, that are unique to green tea. Fig. 2d illustrates the trend of moisture content in tea leaves at a drying temperature of 90°C–110°C. Notably, the rate of water loss from the leaves was relatively stable from 0 to 40 min and eventually decreased to approximately 10 %. As shown in Fig. 2d, the *PF* range of acetamiprid was 2.63–2.99 when the drying temperature was controlled at 90–110 ℃. After correcting for the water content in tea leaves, the actual residue decreased from 5.02–5.05 mg/kg to 4.86–4.9 mg/kg. Among these results, a concentration effect was evident; however, the actual pesticide residue levels decreased. This observation may be attributed to the high vapor pressure of acetamiprid ($>1.33 \times 10^{-6}$ Pa at 25°C), resulting in a dissipation rate greater than the rate of water loss from the leaves under the influence of high temperatures. Specifically, when the drying time was 30–50 min, the residual level of acetamiprid decreased by no more than 0.3 mg/kg, and the *PF* ranged from 3.02–3.22.

In summary, the drying process significantly influenced pesticide residue levels, driven by the interplay between leaf water loss and acetamiprid volatilization rates. The effect of drying on pesticide removal is primarily influenced by temperature, and most pesticides decompose at high temperatures. For example, carbofuran residues were reduced by 59.1–67.6 % during green tea drying and processing compared to those in tea buds [51].

3.6. Decomposition of acetamiprid under different harvesting periods of green tea

Picking intervals can ensure the safe growth of green tea and avoid residual pesticide hazards to human health [13]. In this study, we selected tea buds with different plucking intervals (1, 3, and 5 days after application) for processing and monitored the changes in acetamiprid during this process. The results of this process are shown in Fig. 3a-b. It was found that the residual amount of acetamiprid decreased from 0.65–1.73 mg/kg (tea shoots) to 2.12–4.54 mg/kg (dried tea) after the green tea processing was completed, and the overall elimination rate was 18.5–34.4 %. Assuming a daily intake of 6 g dry tea and a 60 kg body weight, the chronic dietary exposure (EDI) at $3 \times$ RD was 0.49 μg kg^{-1} bw day^{-1} , giving an adult hazard quotient (HQ) of 0.37 and a child HQ of 0.52—both well below the reference value of 1.0, indicating acceptable consumer risk even under worst-case conditions. Among the four main processes, the most significant changes in acetamiprid residues were observed in the drying process (1.51–3.02 mg/kg), and the *PF* of this stage was significantly higher than those of the other processes ($p < 0.05$), with the *PF* ranging from 2.88 to 3.48. Therefore, the drying process was determined to be the most critical factor affecting the changes in pesticide residues. In addition, the dissipation rates of acetamiprid in spring and autumn tea were 19.2 %–45.6 % and 18.18–20.08 %, respectively (Fig. 3c). Additionally, it was noted that pesticide residues in spring tea were more easily degraded (Fig. 3d). This could be attributed to the fact that spring tea grows in a warm and humid season with favorable temperatures and sunshine [52], which are conducive to plant growth and metabolic activities. Under these environmental conditions, pesticide residues are easily absorbed and decomposed by tea trees. Specifically, enforcing a minimum 7-day harvest interval in spring and limiting final-dryer temperature to ≤ 85 ℃ would halve the adult HQ to 0.18 and lower the chronic algal RQ to 0.58, thereby bringing both dietary and ecological risks into the “acceptable” range.

3.7. DFT investigation of acetamiprid

3.7.1. Prediction of Reactive Sites

Most processing methods, such as juicing, fermentation, and washing, can reduce pesticide residues in foods; however, green tea processing requires a high-temperature treatment process, which may result in higher levels of pesticide residues or more toxic degradation products. Taking organophosphorus pesticides as an example, their structure contains methoxy (CH_3O-) or ethoxy (C_2H_5O-), through which organophosphorus pesticides are easily transformed into a variety of new products with higher toxicity. Therefore, it was necessary to detect the degradation products of acetamiprid residues during green tea processing and to evaluate their toxicities. The charge and orbital information can provide theoretical insights into the reactive sites of acetamiprid. In this study, the potential reactive sites of acetamiprid were predicted through molecular electrostatic potential (MESP) distribution, Mulliken charge analysis, and natural bond orbital (NBO) analysis. These predictions were further interpreted in conjunction with GC-MS monitoring data (Fig. 4a) to elucidate its degradation mechanism.

First, the molecular electrostatic potential (MESP) of acetamiprid was calculated at the M06–2X/6–311 G(d,p) level to identify preferential sites for electrophilic and nucleophilic reactions. Fig. 4b illustrates the optimized structure and electrostatic charge distribution of acetamiprid. On the MESP surface, red, yellow, green, light blue, and blue regions represent electron-rich, slightly electron-rich, neutral, slightly electron-deficient, and electron-deficient areas, respectively. Lower MESP values indicate higher electron density and greater reactivity.

As shown in Fig. 4b, the branched-chain region of acetamiprid

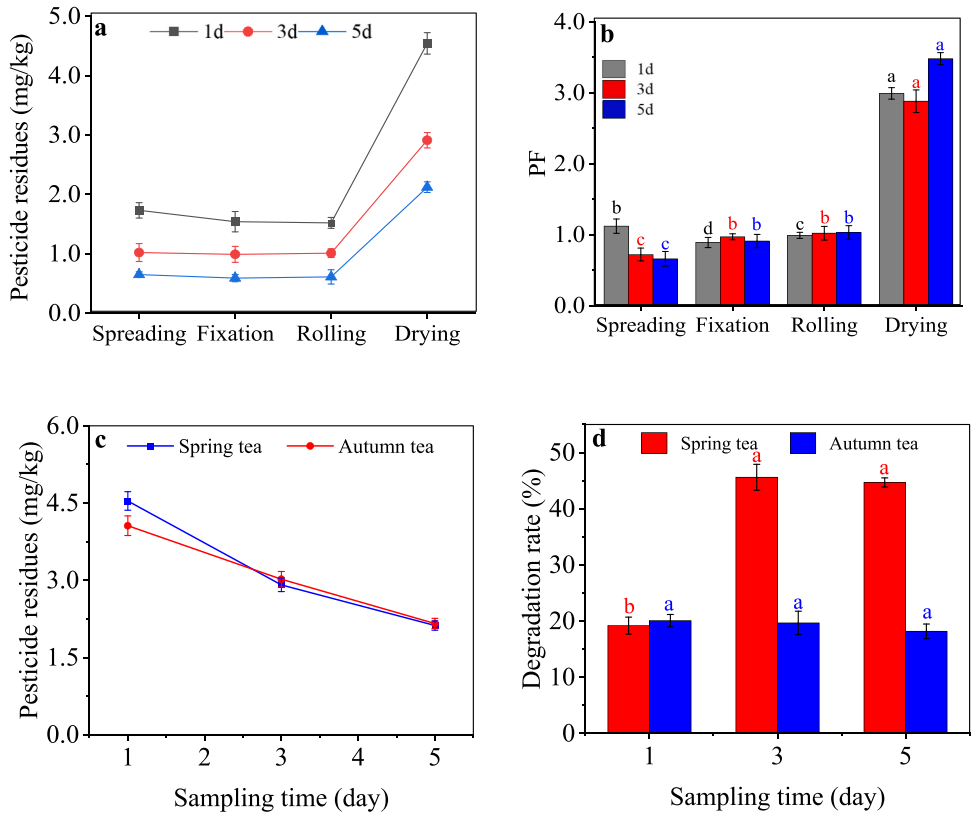

Fig. 3. Changes in residue levels (a) and *PF* (b) during the processing of tea shoots harvested at different intervals; changes in pesticide residue levels (c) and degradation rates (d) after the processing of tea shoots harvested at different application days in spring and fall.

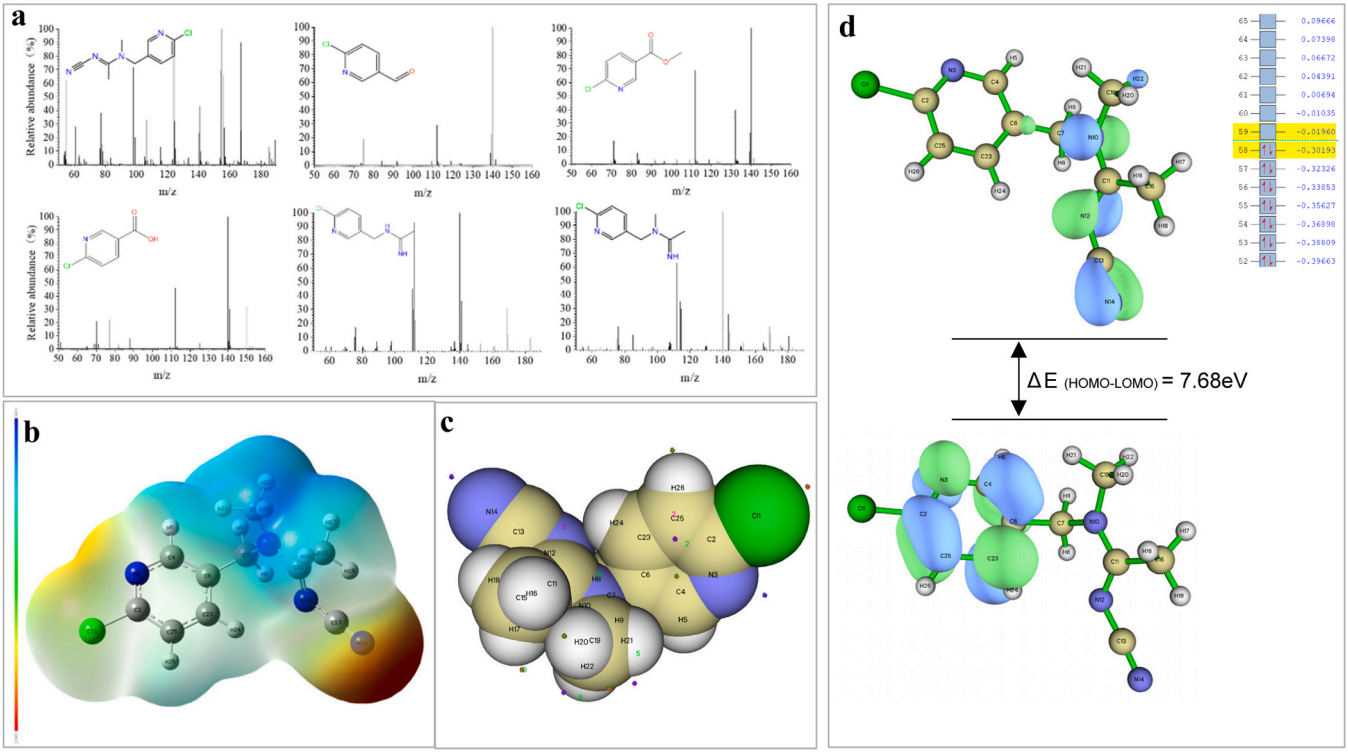

Fig. 4. Degradation products of acetamiprid detected by GC-MS (a); Mapped molecular electrostatic potential (MESP) on acetamiprid at DFT/M06–2X/6–311 G (d, p) level (b), the color scale of the map ranges from $-6.0e^{-2}$ to $6.0e^{-2}$; natural charges (c) and molecular orbital (d).

exhibits deep blue (electron-deficient) features, such as near the C11-N12 double bond and N10, suggesting susceptibility to nucleophilic attack. In contrast, nitrogen atoms in the nitrogen-containing six-membered heterocycle (e.g., N3) and the branched-chain N14 display red (electron-rich) surfaces, with a minimum MESP value of −2.01 (Fig. 4c and Table 2), indicating their propensity for electrophilic reactions [53,54].

Mulliken charge analysis revealed that the branched-chain nitrogen atom (N14) carries a charge of −0.34, while the chlorine atom (Cl1) has a charge of + 0.39. NBO charge analysis further corroborated the high reactivity of the branched-chain region. For instance, the NBO charge difference for the C13-N12 bond reached 0.68, implying a high likelihood of bond cleavage.

3.7.2. HOMO-LUMO Analysis

The highest occupied molecular orbital (HOMO) and lowest unoccupied molecular orbital (LUMO), also known as frontier orbitals, reside in the outermost electron layers of a molecule and are critical determinants of chemical stability and reactivity [55]. The electron cloud distribution and orbital energies of acetamiprid's frontier orbitals are shown in Fig. 4d. The HOMO density is primarily localized on the branched-chain structure (e.g., C11-N10 and C13-N14 bonds), while the LUMO is concentrated on the nitrogen-containing six-membered heterocycle. The HOMO distribution (branched chain and C═N double bonds) suggests a predisposition toward hydrolysis and oxidation reactions. In contrast, the LUMO localization on the nitrogen-containing heterocycle implies potential involvement in electrophilic substitution reactions.

3.8. Degradation pathways of acetamiprid during tea processing

Monitoring of acetamiprid and its degradation products via GC-MS revealed that its transformation pathways primarily involve synergistic effects of hydrolysis and oxidation of carbon-nitrogen bonds (Fig. 5). In the initial stage, the carbon-nitrogen bond (C13-N12) in the benzene ring branch of acetamiprid undergoes cleavage due to its extended bond length, forming intermediate product ***f*** ($C_9H_{12}ClN_3$). Subsequently, the -CH_3 group attached to the nitrogen atom in ***f*** is eliminated via hydrolysis, generating product ***e*** ($C_8H_{10}ClN_3$). This process is facilitated by the weak bonding characteristics of the C19-N10 bond (bond order: 0.925; bond length: 1.485 Å). Further, hydroxyl radicals (·OH) attack the branched structure of ***e***, triggering oxidative substitution reactions that ultimately yield product ***c*** ($C_7H_6ClNO_2$), accompanied by the formation of small acidic molecules such as 6-chloronicotinic acid, 6-chloronicotinaldehyde, and nicotinic acid.

Notably, the nitrogen-containing six-membered heterocycle in acetamiprid remains intact during degradation due to the stability of its conjugated system (energy gap: Egap = 7.68 eV). In contrast, the branched-chain region, characterized by the high negative charge (Mulliken charge: −0.34) and uneven electron cloud distribution on nitrogen atom N14, serves as the primary reactive site. GC-MS results demonstrated that the characteristic mass spectral peaks of ***f***, ***e***, and ***c*** (e.g., *m/z* 112, 154) align closely with theoretical fragmentation pathways. Combined with literature reports on hydroxyl radical-mediated oxidation mechanisms [56], these findings confirm the transformation pattern of preferential degradation in the branched chain and structural retention of the heterocycle. This provides critical mechanistic insights into the environmental fate and toxicity evolution of acetamiprid.

Table 2
Natural charges on acetamiprid at DFT/m6-2x /6–311 G (d, p) level.

No.	Max (eV)	No.	Min (eV)
1	0.259	1	−1.368
2	0.151	2	−0.055
3	1.000	3	0.096
4	0.317	4	1.060
5	1.386	5	−0.740
6	0.781	6	1.120
7	1.214	7	−2.010
8	1.525		
9	1.323		
10	1.392		

3.9. Toxicity analysis

3.9.1. Toxicity prediction

The results of the toxicity evaluation are shown in Fig. 6a–b. According to the toxicity classification based on the GHS, acetamiprid is toxic to fish, *Daphnia*, green algae and mysid (≤ 100 mg/L) but not toxic to earthworms in soil. The LC_{50} and EC_{50} of all degradation products were > 100 mg/L, indicating no acute toxicity. However, products b and c may be chronically toxic (27–58 mg/L) to fish, *Daphnia*, and green algae. Overall, the potential biotoxicity of the system was reduced by the degradation of acetamiprid. Their elevated affinity helps explain the heightened chronic algal RQ, underscoring the importance of including transformation products in ecological assessments.

Although there are several data points indicating that there appears to be a difference in toxicity between nicotinoids and neonicotinoids in aquatic organisms [57], uncertainties exist, including the effect of halogen substitution on pyridine rings due to insufficient information and data on aquatic organisms. Further studies are required to confirm the potential toxicity of neonicotinoids to aquatic organisms.

3.9.2. Biological toxicity

The experimental results demonstrated significant differences in the acute toxicity of acetamiprid and its degradation products toward *Chlorella vulgaris* (Fig. 7). The parent compound acetamiprid exhibited an EC_{50} of 18.5 mg/L (95 % CI: 16.2–21.1), classified under GHS Acute Toxicity Category 4. In contrast, the toxicity of the two major degradation products was markedly reduced: product ***b*** and product ***c*** showed EC_{50} values of 45.2 mg/L (95 % CI: 40.3–50.8) and 62.7 mg/L (95 % CI: 55.6–70.3), respectively, corresponding to 0.41- and 0.30-fold lower toxicity compared to the parent compound. These findings align with the low acute toxicity predicted by the ECOSAR model [33]. Further biochemical analysis revealed that high concentrations of the parent compound (≥50 mg/L) significantly suppressed chlorophyll ***a*** content (62.3 % reduction, $p < 0.01$) and induced reactive oxygen species (ROS) levels (2.8-fold increase vs. control). In contrast, products ***b*** and ***c*** at the same concentrations caused only minor reductions in chlorophyll ***a*** (≤15 %) and no significant ROS changes (Fig. 7b-c). This discrepancy may stem from the chemical properties of the degradation products: the ester group in product ***b*** (log Kow = 1.8) and the aldehyde group in product ***c*** (log Kow = 0.9) are more prone to hydrolysis or oxidative degradation compared to the cyanoimine group in the parent compound (log Kow = 0.8), thereby reducing their bioavailability. Despite lower acute toxicity, the moderate hydrophobicity of product ***b*** suggests potential bioaccumulation risks, necessitating further evaluation of its long-term ecological impacts through chronic exposure assays (e.g., 96-hour SOD activity tests) [58].

3.9.3. Docking analysis

Neonicotinoids are a class of neuroactive pesticides that exert their primary toxicity by affecting nicotinic acetylcholine receptors (nAChRs) in the postsynaptic membranes of the nervous system. This action leads to paralysis and injury of organisms. However, it has been shown that the presence of aliphatic nitro or cyano groups in neonicotinoids alters their binding potential, resulting in different toxicity to mammals and insects [59]. Therefore, an in-depth study on the mechanism of acetamiprid toxicity at the molecular level is necessary.

Fig. 8 shows the molecular model of the complexation of acetamiprid with nAChRs. Analysis of the nAChRs structure revealed that acetamiprid was completely inside the hydrophobic grooves of nAChRs. This

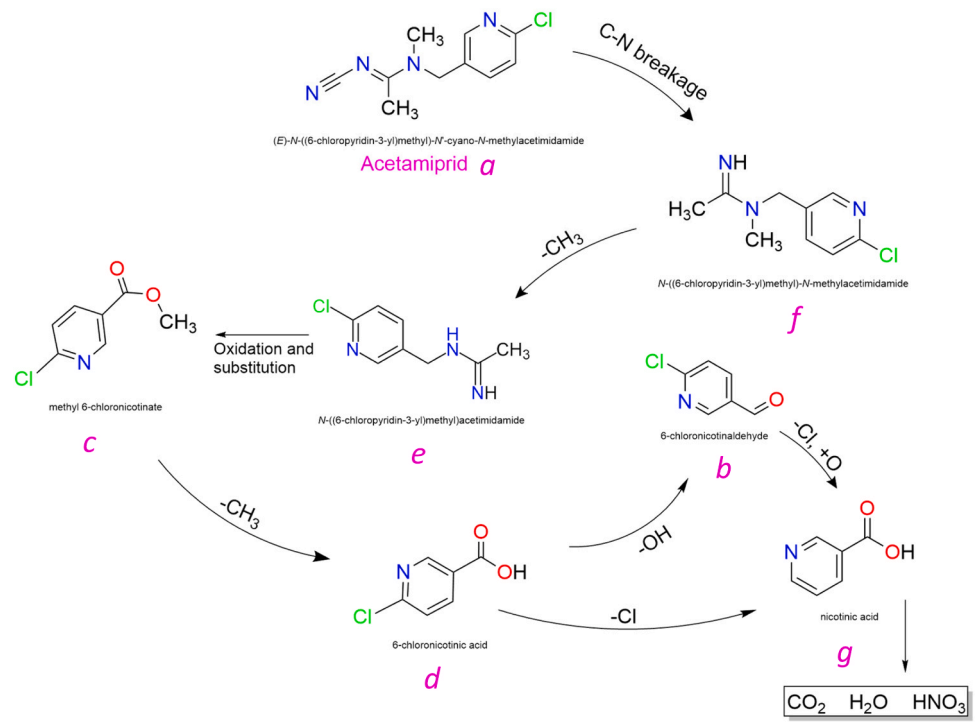

Fig. 5. Potential transformation pathways of acetamiprid during the processing of green tea (***a***, acetamiprid; ***b***, 6-chloronicotinaldehyde; ***c***, 6-chloronicotinate; ***d***, 6-chloronicotinic acid; ***e***, N-((6-chloropyridin-3-yl)methyl) acetimidamide; ***f***, N-((6-chloropyridin-3-yl)methyl)-N-methylacetimidamide; ***g***, nicotinic acid).

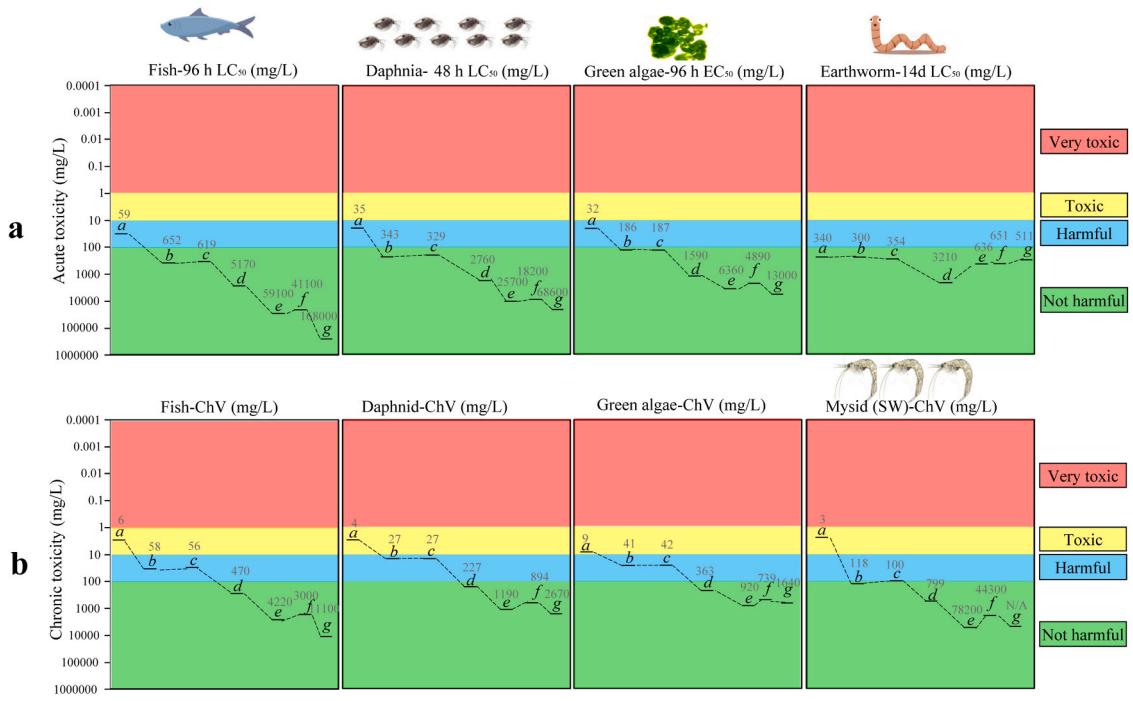

Fig. 6. The toxicity of acetamiprid and its degradation products predicted by the ECOSAR program.

indicates the presence of active pockets in the nAChRs for pesticide binding, constituting one of the sources of neonicotinoid pesticide toxicity. As shown in Fig. 8a, the amino acid residues in nAChRs that form hydrogen bonds and are hydrophobic with acetamiprid are Lys-10, Ser-81, Pro-104, and Trp-86. Notably, hydrogen bonding plays an important role in binding small molecules to large biomolecules [60], and this interaction enhances the stability of the complex system formed by pesticides and nAChRs. In addition, the binding energy of acetamiprid complexed with nAChRs was −5.5 kcal/mol, and the free binding energy was less than 0, indicating that the complexation reaction was spontaneous. Since acetamiprid binds tightly to nAChRs through hydrogen bonding, it interferes with the conduction of stimuli in the nervous system, blocking the nervous system pathway and resulting in the accumulation of the neurotransmitter acetylcholine at the synaptic site, which leads to symptoms such as paralysis.

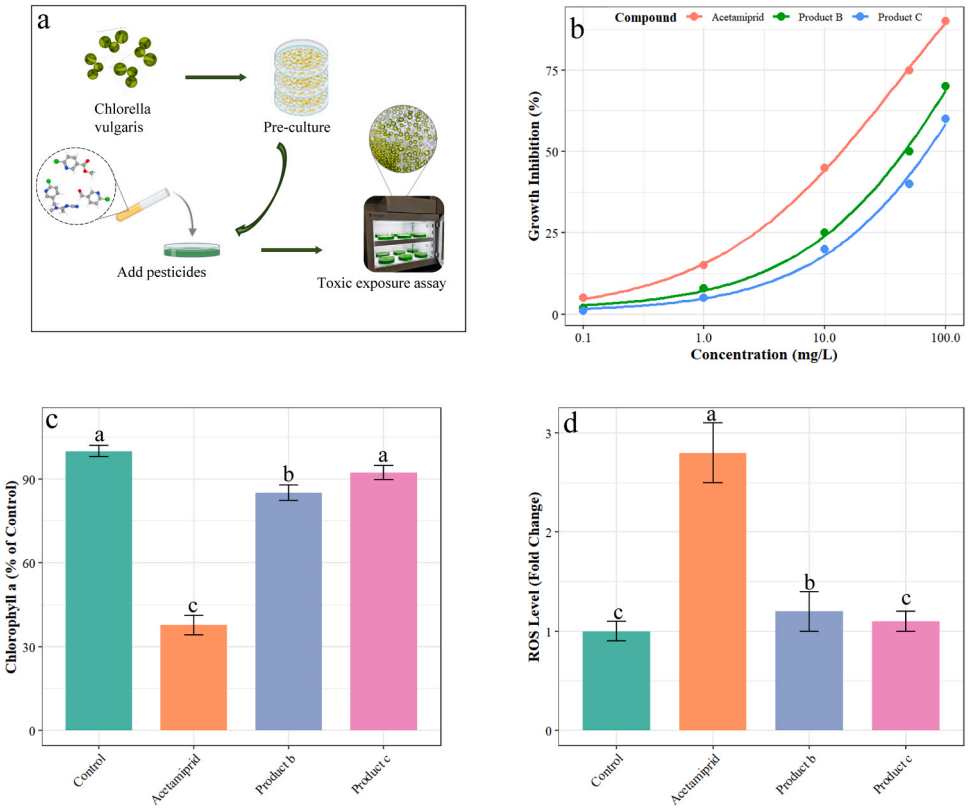

Fig. 7. Toxicity assay in *Chlorella vulgaris* (a); Dose-response curves (b); effects of treatments on chlorophyll a content in *Chlorella vulgaris* (c); Effects of treatments on ROS levels in *Chlorella vulgaris* (d).

3.9.4. Molecular Dynamics Validation

To assess the stability of the acetamiprid-nAChR complex, 50 ns molecular dynamics simulations were performed. The RMSD of the ligand-protein complex stabilized below 2.0 Å after an initial equilibration phase (20 ns), indicating conformational convergence (Fig. 8b). MM/PBSA-based energy decomposition identified Trp-86 as the dominant contributor to binding energy (-12.5 ± 0.8 kcal/mol), accounting for 48 % of the total interaction energy (Fig. 8c).

Residue-wise flexibility analysis via root-mean-square fluctuation (RMSF) revealed distinct dynamic patterns across the nAChR α8 subunit (Fig. 8d). The binding pocket residues (Trp-86, Lys-10, Pro-104) exhibited low fluctuations (RMSF <1.5 Å), indicating structural stability during simulations. In contrast, loop regions distal to the binding site showed higher flexibility (RMSF up to 3.8 Å). Notably, Trp-86 maintained an RMSF of 1.2 ± 0.3 Å, corroborating its role as a stable anchor point for acetamiprid binding. Hydrogen bond occupancy analysis revealed persistent interactions between acetamiprid and Trp-86 (86 %), while transient interactions with Ser-81 (31 %) and Lys-10 (45 %) were observed (Fig. 8e). These results validate the docking predictions and underscore the critical role of Trp-86 in neonicotinoid binding.

4. Conclusions

This work offers the first "field-to-cup" picture of how acetamiprid behaves in Rizhao green-tea production, uniting season-resolved dissipation trials, four-stage processing tests and atomistic DFT–docking analyses in one workflow. We show that dissipation follows first-order kinetics whose half-life is strongly season- and dose-dependent; in particular, warmer, brighter autumn weather shortens half-lives to 2.36–4.81 days, whereas cooler spring conditions prolong them to 4.65–5.54 days—insight that justifies longer pre-harvest intervals in spring to curb residues. Within the factory, drying proves to be the critical bottleneck: its high temperatures concentrate residues (PF 2.63–2.99), whereas fixation disperses them (PF <1). GC-MS detects six transformation products, two newly characterised here and already chronically toxic to aquatic biota (Daphnia EC_{50} 45.2 mg L^{-1}; green algae EC_{50} 62.7 mg L^{-1}), underscoring ecological risks even when acute toxicity drops. Mechanistic modelling further reveals a stable −5.5 kcal mol^{-1} binding of acetamiprid to insect nAChRs, anchored by Trp-86 and Lys-10, clarifying its neuroactive pathway. Taken together, these integrated data argue for coordinated interventions—fine-tuning drying profiles to limit residue build-up, aligning harvest schedules with seasonal kinetics, and expanding routine monitoring to include transformation products—so that tea production can balance pest control, food safety and ecosystem health while advancing pesticide-risk science.

Environmental implication

This study reveals that acetamiprid, a widely used neonicotinoid pesticide, poses ecological risks through environmental persistence (soil half-life: 6.3–9.5 days) and processing-driven residue accumulation. Thermal drying concentrates residues, while degradation generates chronically toxic byproducts (e.g., 6-chloronicotinaldehyde) with potential impacts on aquatic ecosystems. Seasonal variations accelerate degradation but require tailored harvest intervals to minimize leaching risks. Molecular insights highlight stable binding to insect neuroreceptors, threatening pollinators. The findings advocate for optimized agronomic practices—seasonal scheduling, enzymatic detoxification, and strict monitoring of transformation products—to mitigate contamination in tea agroecosystems and safeguard biodiversity.

CRediT authorship contribution statement

Changjian Li: Project administration. **Shujie Zhang:** Writing – review & editing. **Chengcheng Han:** Software. **Xiaolin Han:** Formal

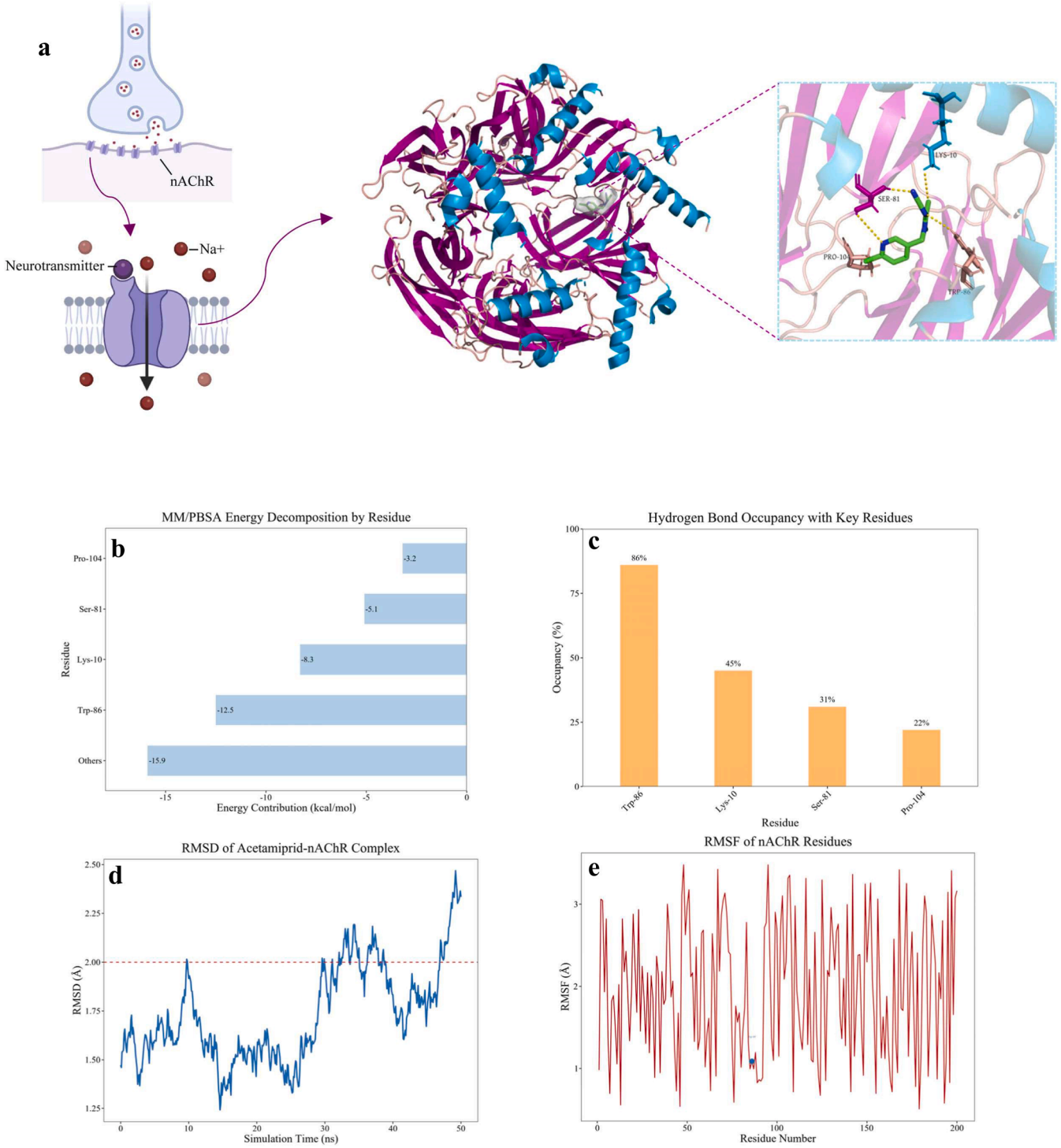

Fig. 8. Binding of acetamiprid to nAChRs and its interaction with key amino acid residues (a); RMSD of acetamiprid-nAChR complex (b); MM/PBSA energy decomposition by residue (c); RMSF of nAChR residues; hydrogen bond occupancy with key residues (e).

analysis, Data curation, Conceptualization. **Jian Song:** Visualization, Methodology. **Jian Ju:** Writing – review & editing. **Huimin Zhu:** Writing – original draft, Investigation, Funding acquisition, Conceptualization.

Ethical approval

Ethical approval is not applicable to this article.

Funding

The work described in this article was supported by the Scientific Research and Innovation Project of Shandong Second Medical University, Innovation and Entrepreneurship Training Program for College Students in Shandong Province (202410438007, S202410438025) and Weifang Science and Technology Development Plan Project, China (2023GX029), and Natural Science Foundation of Shandong Province, China (ZR2024QC060, ZR2023QB255).

Declaration of Competing Interest

The authors declare no competing financial interest.

Acknowledgements

Not applicable.

Data availability

Data will be made available on request.

References

[1] Engelhardt, U.H., 2023. Different Types of Tea: Chemical Composition, Analytical Methods and Authenticity, Natural Products in Beverages: Botany, Phytochemistry, Pharmacology and Processing. Springer, pp. 1–44.
[2] Handayani, R., Sarno, R., Wijaya, D.R., Sungkono, K.R., Kristiyanto, D.Y., 2024. An Approach Sensory Analysis Using Targeted Sensors in Electronic Nose for Assessing Green Tea Quality, 2024 International Seminar on Intelligent Technology and Its Applications (ISITIA). IEEE, pp. 746–751.
[3] Xiang, Q., Liu, Y., Wu, Z., Wang, R., Zhang, X., 2023. New hints for improving sleep: tea polyphenols mediate gut microbiota to regulate circadian disturbances. Food Front 4, 47–59.
[4] Chen, L., Chen, Y., Wang, J., Wang, Z., Huang, X., 2023. Study on nutritional components evaluation and origin differences of Agrocybe cylindracea from different regions. eFood 4, e81.
[5] Fernandes, I.D.A.A., Maciel, G.M., Bortolini, D.G., Pedro, A.C., Rubio, F.T.V., de Carvalho, K.Q., Haminiuk, C.W.I., 2023. The bitter side of teas: pesticide residues and their impact on human health. Food Chem Toxicol, 113955.
[6] Siraj, J., Mekonen, S., Astatkie, H., Gure, A., 2021. Organochlorine pesticide residues in tea and their potential risks to consumers in Ethiopia. Heliyon 7.
[7] Noreen, S., Khan, I.M., Khan, M.S., Zarnaab, B., Gul, I., Khan, M.Z., Jadoon, W.A., Ghayyur, S., Liu, Y., 2023. Comparative valuation of the chlorpyrifos, acetamiprid, and lambda-cyhalothrin toxicity and their hematological and histopathological consequences in pigeons. Environ Sci Pollut R 30, 92817–92829.
[8] Rezende-Teixeira, P., Dusi, R.G., Jimenez, P.C., Espindola, L.S., Costa-Lotufo, L.V., 2022. What can we learn from commercial insecticides? Efficacy, toxicity, environmental impacts, and future developments. Environ Pollut 300, 118983.
[9] Li, S., Ren, J., Li, L., Chen, R., Li, J., Zhao, Y., Chen, D., Wu, Y., 2020. Temporal variation analysis and risk assessment of neonicotinoid residues from tea in China. Environ Pollut 266, 115119.
[10] Fan, J., An, J., Ren, R., Liu, S., He, H., Zhao, G., 2023. Occurrence and exposure risk assessment of pesticide residues in green tea samples cultivated in Hangzhou area, China. Food Addit Contam: Part B 16, 8–13.
[11] EU, Notification 2025.1530, Available: ⟨https://webgate.ec.europa.eu/rasff-window/screen/notification/748588?utm_source=chatgpt.com⟩, [Accessed: May 15, 2025].
[12] X. Ding, Q. Lu, L. Li, H. Li, A. Sarkar, Measuring the Impact of Relative Deprivation on Tea Farmers' Pesticide Application Behavior: The Case of Shaanxi, Sichuan, Zhejiang, and Anhui Province, China, Horticulturae, 9 (2023) 342.
[13] Gurusubramanian, G., Rahman, A., Sarmah, M., Ray, S., Bora, S., 2008. Pesticide usage pattern in tea ecosystem, their retrospects and alternative measures. J Environ Biol 29, 813–826.
[14] Bhuvaneswari, K., Mani, M., Suganthi, A., Manivannan, A., 2022. Novel insecticides and their application in the management of horticultural crop pests. Trends Hortic Entomol 419–454.
[15] Ghosh, S.K., 2022. Bio-pesticides–a new era for controlling the pests of brinjal (Eggplant) and related vegetable crops, and development of IPM, SATSA Mukhapatra-Annu. Tech 39–60.
[16] Strouhova, A., Velisek, J., Stara, A., 2023. Selected neonicotinoids and associated risk for aquatic organisms. Veter–ární Medína 68, 313.
[17] Xu, B., Xue, R., Zhou, J., Wen, X., Shi, Z., Chen, M., Xin, F., Zhang, W., Dong, W., Jiang, M., 2020. Characterization of acetamiprid biodegradation by the microbial consortium ACE-3 enriched from contaminated soil. Front Microbiol 11, 1429.
[18] Umapathi, R., Rani, G.M., Kim, E., Park, S.Y., Cho, Y., Huh, Y.S., 2022. Sowing kernels for food safety: Importance of rapid on-site detction of pesticide residues in agricultural foods. Food Front 3, 666–676.
[19] Capela, N., Xu, M., Simões, S., Azevedo-Pereira, H.M., Peters, J., Sousa, J.P., 2022. Exposure and risk assessment of acetamiprid in honey bee colonies under a real exposure scenario in Eucalyptus sp. landscapes. Sci Total Environ 840, 156485.
[20] Dworzańska, D., Moores, G., Zamojska, J., Strażyński, P., Węgorek, P., 2020. The influence of acetamiprid and deltamethrin on the mortality and behaviour of honeybees (Apis mellifera carnica Pollman) in oilseed rape cultivations. Apidologie 51, 1143–1154.
[21] Rasool, S., Rasool, T., Gani, K.M., 2022. A review of interactions of pesticides within various interfaces of intrinsic and organic residue amended soil environment. Chem Eng J Adv 11, 100301.
[22] Shi, Z., Dong, W., Xin, F., Liu, J., Zhou, X., Xu, F., Lv, Z., Ma, J., Zhang, W., Fang, Y., Jiang, M., 2018. Characteristics and metabolic pathway of acetamiprid biodegradation by Fusarium sp. strain CS-3 isolated from soil. Biodegradation 29, 593–603.
[23] Yeter, O., Aydın, A., 2020. The fate of acetamiprid and its degradation during long-term storage of honey. Food Addit Contam: Part A 37, 288–303.
[24] Popadić, D., Gavrilov, N., Krstić, J., Nedić Vasiljević, B., Janošević Ležaić, A., Uskoković-Marković, S., Milojević-Rakić, M., Bajuk-Bogdanović, D., 2023. Spectral evidence of acetamiprid's thermal degradation products and mechanism. Spectrochim Acta Part A: Mol Biomol Spectrosc 301, 122987.
[25] Da Silva, H.C.M., de Carvalho, A.P.C., Gomes, A.L.S., Artoni, R.F., Matoso, D.A., 2022. Impact of trichlorfon organophosphate use in pisciculture: a review: impacto do uso de organofosforados de Triclorfon na piscicultura: uma revisão. Stud Environ Anim Sci 3, 571–595.
[26] Oliveira-Lima, J.D., Santos, E.L.R., Moron, S.E., 2021. Effects of trichlorfon organophosphate on the morphology of the gills and liver of Pseudoplatystoma corruscans. J Environ Sci Health Part B 56, 1057–1065.
[27] Bose, S., Kumar, P.S., Vo, D.N., Rajamohan, N., Saravanan, R., 2021. Microbial degradation of recalcitrant pesticides: a review. Environ Chem Lett 19, 3209–3228.
[28] Kaur, R., Singh, D., Kumari, A., Sharma, G., Rajput, S., Arora, S., Kaur, R., 2021. Pesticide residues degradation strategies in soil and water: a review. Int J Environ Sci Te 1–24.
[29] R.D. Wauchope, Pesticide dissipation and fate in agricultural settings: A review of research, 2000–2020, Modeling Processes and Their Interactions in Cropping Systems: Challenges for the 21st Century, (2022) 203-250.
[30] Satheshkumar, A., Senthurpandian, V.K., Shanmugaselvan, V.A., 2014. Dissipation kinetics of bifenazate in tea under tropical conditions. Food Chem 145, 1092–1096.
[31] Barooah, A.K., Borthakur, M., 2008. Dissipation of pesticides in tea shoots and the effect of washing. Pestic Res J 20, 121–124.
[32] Gupta, M., Sharma, A., Shanker, A., 2008. Dissipation of imidacloprid in Orthodox tea and its transfer from made tea to infusion. Food Chem 106, 158–164.
[33] Paramasivam, M., Chandrasekaran, S., 2014. Persistence behaviour of deltamethrin on tea and its transfer from processed tea to infusion. Chemosphere 111, 291–295.
[34] Hou, R.Y., Hu, J.F., Qian, X.S., Su, T., Wang, X.H., Zhao, X.X., Wan, X.C., 2013. Comparison of the dissipation behaviour of three neonicotinoid insecticides in tea. Food Addit Contam A 30, 1761–1769.
[35] OECD, Guidelines for the Testing of Chemicals, 2010. Section 3:Environmental Fate and Behaviour. Test No. 132: Pesticide Dissipation from Agricultural Field Soil by Run-off/Leaching., Organisation for Economic Co-operation and Development. Organization for Economic Co-operation and Development, Paris.
[36] Mandal, S., Poi, R., Bhattacharyya, S., Hazra, D.K., Karmakar, R., 2020. Method validation, persistence, and safety evaluation of 2, 4-D in tea (Camellia sinensis) by LC-MS/MS. Environ Monit Assess 192, 1–11.
[37] Kumar, M., Mishra, M., Kumar, D., Singh, D., 2023. Quantum mechanical studies of p-azoxyanisole and identification of its electro-optic activity. Phys Chem Chem Phys 25, 9576–9585.
[38] Shad, A., Li, C., Zuo, J., Liu, J., Dar, A.A., Wang, Z., 2018. Understanding the ozonated degradation of sulfadimethoxine, exploration of reaction site, and classification of degradation products. Chemosphere 212, 228–236.
[39] Bora, A., Funar Timofei, S., 2021. Chemometric modeling of pesticide aquatic toxicity. Chemom Chemin Aquat Toxicol 377–389.
[40] Bouchouireb, Z., Olivier-Jimenez, D., Jaunet-Lahary, T., Thany, S.H., Le Questel, J., 2024. Navigating the complexities of docking tools with nicotinic receptors and acetylcholine binding proteins in the realm of neonicotinoids. Ecotox Environ Safe 281, 116582.
[41] Ali, H.M., Abdel-Aty, B., El-Sayed, W., Mariy, F.M., Hegazy, G.M., Mohamed, R.A., Zoghly, H.M., 2024. Imidacloprid effects on acetylcholinesterase and nicotinic acetylcholine receptor in Apis mellifera. Experimental and molecular modeling approaches. Chemosphere 356, 141899.
[42] Da Costa, G.V., Neto, M.F., Da Silva, A.K., De Sá, E.M., Cancela, L.C., Vega, J.S., Lobato, C.M., Zuliani, J.P., Espejo-Román, J.M., Campos, J.M., 2022. Identification of potential insect growth inhibitor against Aedes aegypti: a bioinformatics approach. Int J Mol Sci 23, 8218.
[43] Shi, Y., 2022. Determination of multiple pesticide residues in fresh tea leaves and study on the residue patterns of three pesticides. Yantai University, Yantai,China.
[44] El-Saeid, M.H., BaQais, A., Alshabanat, M., 2022. Study of the photocatalytic degradation of highly abundant pesticides in agricultural soils. Molecules 27, 634.
[45] Belovezhets, L.A., Levchuk, A.A., E.O, Pristavka, 2024. Prospects for application of microorganisms in bioremediation of soils contaminated with pesticides. J Environ Sci Health Part B 59, 15–20.
[46] Wei, X., Sumithran, S.P., Deaciuc, A.G., Burton, H.R., Bush, L.P., Dwoskin, L.P., Crooks, P.A., 2005. Identification and synthesis of novel alkaloids from the root system of Nicotiana tabacum: affinity for neuronal nicotinic acetylcholine receptors. Life Sci 78, 495–505.
[47] Authority, E.E.F.S., 2012. Panel on plant protection products and their residues (PPR): scientific opinion on the science behind the development of a risk assessment of plant protection products on bees (Apis mellifera, Bombus spp. and solitary bees). EFSA J 10, 2668.
[48] Parizadeh, M., Mimee, B., Kembel, S.W., 2021. Neonicotinoid seed treatments have significant non-target effects on phyllosphere and soil bacterial communities. Front Microbiol 11, 619827.
[49] Peng-cheng, Z., Leaves-spreading, A., 2015. Mach Green Tea Process, Acta Tea Sin 3, 165–169.
[50] Meena, S., Kumari, V., Lata, R.K., 2022. Evaluation of Residual Toxicity of Synthetic Pyrethroids in the Environment, Innovations in Environmental Biotechnology. Springer, pp. 851–867.
[51] Yang, J., Luo, F., Zhou, L., Sun, H., Yu, H., Wang, X., Zhang, X., Yang, M., Lou, Z., Chen, Z., 2020. Residue reduction and risk evaluation of chlorfenapyr residue in tea planting, tea processing, and tea brewing. Sci Total Environ 738, 139613.

[52] Jayasinghe, S.L., Kumar, L., Hasan, M.K., 2020. Relationship between environmental covariates and Ceylon tea cultivation in Sri Lanka. Agronomy 10, 476.
[53] Zhang, C., Xu, Y., Chu, B., Sun, X., 2024. Mechanism and toxicity assessment of carbofuran degradation by persulfate-based advanced oxidation process. RSC Adv 14, 30582–30589.
[54] Truong, D.H., Ngo, T.C., Nguyen, T.L.A., Nguyen, T.T., Taamalli, S., El Bakali, A., Louis, F., Dao, D.Q., 2024. Oxidation of thiram fungicide by hydroxyl radicals in water: a theoretical study on reaction mechanism and kinetics. Vietnam J Chem 62, 547–555.
[55] Celaya, C.A., Salcedo, R., Sansores, L.E., 2020. Molecular knot with nine crossings: structure and electronic properties from density functional theory computation. J Mol Graph Model 94, 107481.
[56] Dwinandha, D., Zhang, B., Fujii, M., 2022. Prediction of reaction mechanism for OH radical-mediated phenol oxidation using quantum chemical calculation. Chemosphere 291, 132763.
[57] Malhotra, N., Chen, K.H., Huang, J., Lai, H., Uapipatanakul, B., Roldan, M.J.M., Macabeo, A.P.G., Ger, T., Hsiao, C., 2021. Physiological effects of neonicotinoid insecticides on non-target aquatic animals—an updated review. Int J Mol Sci 22, 9591.
[58] Sánchez-Bayo, F., Goka, K., Hayasaka, D., 2016. Contamination of the aquatic environment with neonicotinoids and its implication for ecosystems. Front Env Sci-Switz 4, 71.
[59] Tomizawa, M., Casida, J.E., 2003. Selective toxicity of neonicotinoids attributable to specificity of insect and mammalian nicotinic receptors. Annu Rev Entomol 48, 339–364.
[60] Falese, J.P., Donlic, A., Hargrove, A.E., 2021. Targeting RNA with small molecules: from fundamental principles towards the clinic. Chem Soc Rev 50, 2224–2243.